

# Enhanced Atrial Fibrillation Detection-based Wavelet Scattering Transform with Time Window Selection and Neural Network Integration

Mohamed Elmehdi Ait Bourkha<sup>1\*</sup>, Anas Hatim<sup>2</sup>, Dounia Nasir<sup>3</sup>, Said El Beid<sup>4</sup>

Information Technology and Modeling Team (TIM), National School of Applied Sciences (ENSA) of Marrakech,  
Cadi Ayyad University (UCA), Marrakech, Morocco<sup>1, 2, 3</sup>

Control and Computing for Smart Systems and Green Energy (CISIEV), ENSA of Marrakech, UCA, Marrakech, Morocco<sup>4</sup>

**Abstract**—Atrial Fibrillation (AF), a prevalent anomaly in cardiac rhythm, significantly impacts a substantial portion of the population, with projections indicating an escalation in its prevalence in the near future. This disorder manifests as irregular and accelerated heartbeats originating within the heart's upper chambers known as the atria. Neglecting to address this condition could potentially lead to serious consequences, particularly an elevated susceptibility to stroke and heart failure. This underscores the critical importance of developing an automated approach for detecting AF. In our study, an automatic approach was introduced for classifying short single-lead Electrocardiogram (ECG) recordings signals into four categories: Atrial fibrillation (AF), Normal rhythm (N), Noisy rhythm (~), or Other rhythms (O). The wavelet scattering network (WSN) is employed to extract morphological features from the ECG signals, which are then inputted into an Artificial Neural Network (ANN) with time windows selection and majority vote. The results from the testing data exhibit that our proposed model outperforms the state-of-art models, achieving a remarkable overall accuracy of 87.35% and an F1 score of 89.13%.

**Keywords**—*Electrocardiogram (ECG); Atrial Fibrillation (AF); Wavelet Scattering Network (WSN); Artificial Neural Network (ANN)*

## I. INTRODUCTION

The ECG is a recording of electrical potential differences on the body surface that result from the electrical activity in the heart [1]. An ECG is produced when a nerve impulse stimulates the heart, causing a current to spread across the body's surface. This current creates a voltage drop ranging from a few microvolts to millivolts, accompanied by variations in the impulse. Typically, these impulses have very low amplitude, necessitating thousands of times of amplification [2]. The ECG is typically a voltmeter that uses up to 12 different leads (electrodes) placed on designated areas of the body [3].

Because of its straightforwardness and non-intrusive characteristics, the ECG has been extensively utilized in the identification of heart diseases [4]. The detection of heart diseases typically involves the analysis of ECG signals, which unveil irregularities commonly known as arrhythmias. These manifestations signify deviations from a regular heart rhythm, potentially causing irregular or abnormal heartbeats, often

experienced as palpitations. Arrhythmias are broadly categorized into two main types: ventricular and supraventricular. Atrial Fibrillation (AF), a prevalent condition, falls under the category of supraventricular arrhythmias due to its origination within the heart's upper chambers, the atria. In contrast, ventricular arrhythmias arise from the heart's lower chambers or ventricles. Understanding this differentiation is crucial for accurately identifying and subsequently treating various forms of arrhythmias. This distinction aids medical professionals in precisely classifying the type of arrhythmia observed in a patient, paving the way for more targeted and effective treatment strategies.

Early identification plays a pivotal role in addressing heart arrhythmias, potentially offering significant opportunities to save lives. Utilizing the ECG as a primary diagnostic tool becomes essential in achieving this imperative objective [5]. Nevertheless, the manual interpretation of prolonged ECG recordings introduces a multitude of escalating challenges. As these recordings extend in duration, the intricacies grow, rendering the process more time-consuming, intricate, and arduous. The exhaustive review demanded by these extended recordings not only prolongs the analysis but also heightens the complexity of the interpretation process, making it more challenging [6]. In response to these challenges, cardiologists turn to automated diagnostic algorithms, which streamline the analysis of extensive ECG data [7]. This incorporation of automated methodologies proves to be an invaluable solution, offering a streamlined approach to overcome the hurdles associated with manual interpretation. Consequently, the utilization of these automated tools not only enhances efficiency but significantly improves the precision and management of prolonged ECG recordings. Numerous research initiatives have concentrated on employing classical machine learning models to identify arrhythmias within ECG signals. These models have shown efficacy in analyzing both short-term and long-term ECG readings, primarily focusing on the scrutiny of individual heartbeats within the signal [8-9]. Nevertheless, these models require feature engineering and domain expertise, introducing aspects that are time-consuming and demanding. To address these challenges, deep learning models like Convolutional Neural Networks (CNN) and Long Short-Term Neural Networks have emerged, showcasing impressive performance in detecting arrhythmias [10-11].

AF is the prevailing prolonged cardiac irregularity, found in around 1-2% of the overall population [12-13]. This condition carries notable implications for both mortality and morbidity due to its strong links with various health risks. Individuals with AF face an increased likelihood of experiencing severe outcomes, including stroke, hospitalization, heart failure, and coronary artery disease. The association of AF with these risks underscores its profound impact on cardiovascular health [13-14]. AF's connection to an elevated risk of death further underscores its significance. The irregular heartbeat pattern in AF can lead to blood clots forming within the atria, which might subsequently travel to the brain, causing a stroke. Additionally, the erratic heart rhythm can strain the heart's function over time, potentially culminating in heart failure.

AF impacts more than 12 million people in Europe and North America, and this number is expected to triple in the next 30-50 years. This escalating prevalence underscores the need for increased efforts in diagnosis, treatment, and management to address the growing public health challenge [15]. More notably, AF becomes more common as individuals age. For those between 40-50 years old, the incidence is under 0.5%, while among those 80 and older, it ranges from 5-15%. This age-related rise in AF highlights the need for targeted monitoring and interventions to address the growing risk in the elderly [16]. Recognizing this trend, a multitude of research works and papers have emerged, aiming to develop automatic models utilizing Machine Learning (ML) techniques and Deep Learning (DL) [17]. These endeavors aim to facilitate the diagnosis and early detection of AF, potentially saving the lives of millions across the globe.

In the following sections of this paper, related works were explored, specifically focusing on Automated AF systems from previous endeavors in Section II. Subsequently, our materials and methods cover a data description, data preprocessing, and the features extraction method in Section III. A detailed account was presented to explain the classification model used and the evaluation metrics applied. Further Section IV encompasses the results, where our findings were analyzed and described. The discussion section follows, where our results were compared with existing automated AF detection models. Lastly, the conclusion summarizes our findings, outlines limitations, and suggests avenues for future research in Section V.

## II. RELATED WORKS

In this paper, a comparison was conducted with state-of-art models designed for AF detection. Notably, Garcia et al. [18] introduced a method that utilizes surface ECG data, capturing variability in ventricular and atrial activities. The approach involves generating time series data from R\_R intervals and morphological features of fibrillatory waves in T\_Q intervals. The regularity of these time series is quantified using the Coefficient of Sample Entropy (COSEn), and a multi-class Support Vector Machine (SVM) distinguishes between AF, N and O. Their algorithm underwent validation in the PhysioNet Computing in Cardiology Challenge 2017.

Rajpurkar et al. [19] introduced an algorithm surpassing board-certified cardiologist's proficiency, exhibiting exceptional accuracy in detecting a wide range of heart

arrhythmias. The algorithm excels by applying to single-lead wearable monitor electrocardiograms. A sophisticated 34-layer CNN is crucial in mapping ECG sequences to rhythm classes. The study includes a gold standard test set annotated by board-certified cardiologists, serving as a benchmark where the algorithm outperforms individual cardiologists in both recall and precision.

Coppola et al. [20] introduced a data-driven model for automated AF detection from a single ECG lead. The model incorporates features such as heart rate variability, spectral power analysis, and statistical modeling to capture atrial activity nuances. Employing an over-sampling strategy for dataset balance, they crafted a hierarchical classification model predicting ECG signals into AF, N, noise interference or O. Their approach includes a hierarchical bagged ensemble classifier, achieving an average F1 score of 0.7855%.

Makinckas et al. [21] introduced a paradigm utilizing a Long Short Term Memory (LSTM) network, a neural architecture efficiently learning patterns from pre-computed QRS complex features for ECG signal classification. Despite its classification as a deep neural network, their architecture, with a mere 1791 parameters, achieves a remarkable balance between complexity and efficiency. The crux of their methodology lies in the LSTM network's unique ability to comprehend patterns in QRS complex features, facilitating accurate categorization of diverse ECG signals. Their LSTM based model demonstrated effectiveness with a commendable final challenge F1 score of 78% across N, AF, O and ~.

Schwab et al. [22] utilized a richly annotated dataset of 12,186 single-lead ECG recordings. Their approach involved constructing a diverse ensemble of Recurrent Neural Networks (RNN) proficient in discerning differences among N, AF, O, and ~. To enhance temporal learning, they introduced a novel task formulation leveraging ECG signal segmentation into heartbeats, reducing time steps per sequence significantly. Incorporating an attention mechanism further augmented their RNN, enabling the model to focus on specific heartbeats for decision-making. With attention mechanisms, their model achieved an average F1 score of 79%.

Andreotti et al. [23] classified ECG segments into AF, N, O and ~. They conducted a comparative analysis, pitting a feature based classifier against a CNN. Both were meticulously trained on challenge data and augmented with Physionet database. The feature based classifier achieved a 72.0% F1 score during training and 79% on the hidden test set. Meanwhile, the CNN scored 72.1% on the augmented database and 83% on the test set, resulting in a final score of 79%.

Jiménez-Serrano et al. [24] integrated a Feedforward Neural Network (FFNN) for classifying short single-lead ECG segments into N, AF, O and ~. Extracting 72 features from ventricular activity in 8528 ECG records, they conducted a meticulous Feature Selection (FS) process and a detailed grid search for FFNN training parameters. Filtering down to 50 features during FS improved the initial F1 score from 70% to 73%. The FFNN model achieved a final F1 score of 77 % on test data, demonstrating its efficacy in discriminating ECG patterns.

Pandey et al. [25] analyzed ECG data from PhysioNet/CinC Challenge 2017, aiming to differentiate cardiac rhythms, particularly AF, N, O and ~. Their approach combined traditional machine learning with deep neural networks, integrating a Residual Network (ResNet), CNN, Bidirectional LSTM (BiLSTM), and Radial Basis Function (RBF) neural network. The hybrid model achieved an F1 score of 80% and an accuracy of 85% in discerning AF rhythms within the ECG data.

Clifford et al. [26] utilized PhysioNet/CinC Challenge 2017 to distinguish AF from ~, N, or O in short-term ECG recordings. The extensive dataset included 12,186 ECGs, with 8,528 in the public training set and 3,658 in the hidden test set. Utilizing a combination of 45 algorithms, incorporating the LASSO technique, they achieved an F1 score of 86%.

While numerous related works have attempted to detect AF through diverse techniques, including ML, DL, and hybrid models, the prediction accuracy remains notably low. The highest F1 score, achieved by Clifford et al. [26] was 86%, underscores the significance of developing a new approach to enhance the accuracy of AF detection.

### III. MATERIALS AND METHODS

#### A. Database Description

The research utilizes a publicly available database accessible through this link (<https://archive.physionet.org/pn3/challenge/2017/>).

This database comprises 8,528 ECG recordings, which were made available as a public training set for utilization in the 2017 PhysioNet/Computing in cardiology challenge, Table I show the distribution of each class label of the dataset [27]. These recordings were captured using an AliveCor handheld device, which automatically uploads the recordings via a mobile phone application. The dataset includes both these recordings and an additional 3,658 recordings retained as a concealed test set. AliveCor provided these recordings for the Challenge. Each ECG recording was sampled at 300 Hz and underwent band-pass filtration through the AliveCor device.

TABLE I. CLASS LABELS DISTRIBUTION

Class Label	No. Instances
N	5050
AF	738
O	2456
~	284

#### B. Data Preprocessing

The challenge's dataset draws from a particular database. To ensure a fair basis for comparison with earlier studies that utilized a 20-second interval, each ECG recording was divided into segments. This approach was adopted to establish a uniform time window for analysis, in accordance with previous research practices. Furthermore, the dataset exhibited an imbalance, which could pose training challenges leading to inaccurate classification outcomes. To address this, the Synthetic Minority Over Sampling Technique (SMOTE) was

employed [28]. SMOTE generates synthetic instances of the minority class to rebalance the data and enhance classification performance.

Following the application of the SMOTE technique on the 8,528 ECG recordings with segmentations, our dataset was transformed, resulting in 18829 ECG segments. The successful application of SMOTE effectively balanced the class distribution. This balance is pivotal, as it enables the model to achieve precise classification outcomes and effectively differentiate among the four distinct classes. As a consequence of this enhanced discriminatory capacity, our approach will yield elevated accuracy and F1 score results.

In Fig. 1, an ECG segment depicting AF is observed. Notably, the absence of a consistent sinus rhythm is evident through variable R\_R intervals. Additionally, the ECG waveform reflects the absence of certain P waves, confirming the presence of AF.

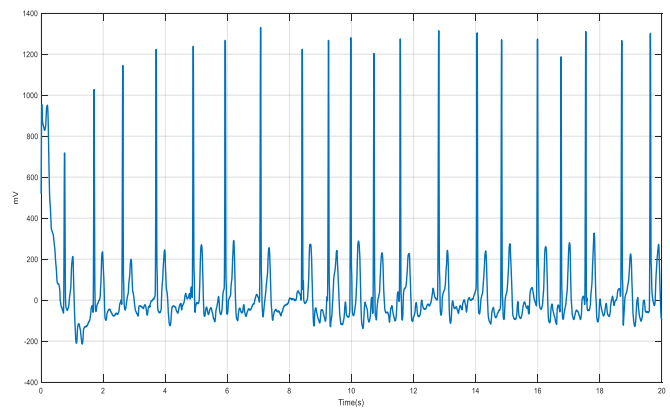


Fig. 1. ECG with atrial fibrillation.

Fig. 2 displays an ECG segment with a normal rhythm. The fixed R\_R interval and the presence of all waves and complexes in the ECG waveform are noticeable, indicating the normalcy of the ECG segment.

Fig. 3 reveals an ECG segment with a variable R\_R interval, signifying that the ECG segments cannot be classified as N. Notably, the presence of P waves in each ECG heartbeat suggests a deviation from AF. Instead, this ECG segment is categorized as another rhythm.

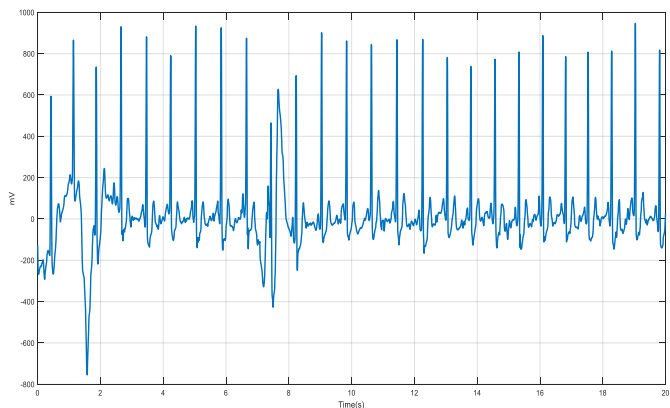


Fig. 2. ECG with normal rhythm.

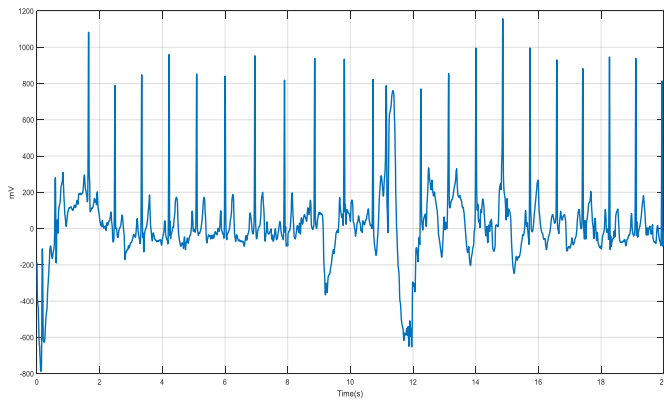


Fig. 3. ECG with other rhythm.

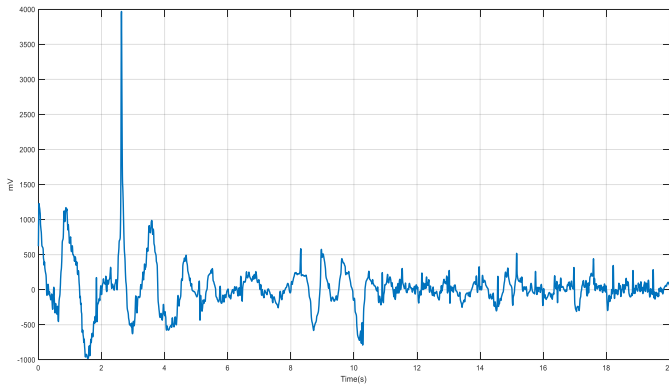


Fig. 4. ECG with noise.

Fig. 4 highlights the absence of identifiable waves or complexes in the ECG segment waveform, indicating that this ECG segment is noisy.

After addressing the imbalance in the dataset through the application of SMOTE, the data was divided into two distinct parts, employing an 80-20% split ratio. This division was carried out with a stratified approach, ensuring that each class label was proportionally represented in both the training and testing sets. Specifically, 80% of the data from each class was allocated to the training set, while the remaining 20% was set aside for testing purposes, which results in a total of 3764 ECG segments for testing and 15065 ECG segments for training. To further enhance the robustness of the model, the training set, constituting 80% of the data, underwent an evaluation process using a five-fold cross-validation technique. This technique involved partitioning the training data into five subsets, training the model on four of these subsets while using the 5<sup>th</sup> for validation, and then rotating the subsets iteratively. This meticulous combination of techniques facilitated the creation of a well-generalized model capable of effectively addressing the initial data imbalance and yielding reliable performance results.

### C. Features Extraction

In this paper, the potential of the WSN was harnessed to meticulously extract an array of intricate morphological characteristics from ECG segments. The wavelet scattering approach is a distinguished member of the deep convolution

network family crafted for signal processing, that serve as the linchpin for capturing multifaceted information.

What sets the wavelet scattering method apart is its unique capacity to seamlessly navigate through both the time and frequency domains of signals. By employing wavelets as the foundational building blocks, the network inherently grasps both the rapid fluctuations occurring in short time spans and the nuanced oscillatory patterns occurring over varied frequency ranges. The WSN provides features with translation and rotation invariance, making it suitable for image and audio analysis [29]. It offers stable features for denoising and enables dimensionality reduction for enhanced accuracy.

In this paper, the WSN with Gabor wavelets is utilized due to their morphological similarity to the QRS complex, making them suitable for extracting features from ECG segments [30]. The definition of a Gabor wavelet in Eq. (1) involves the multiplication of a Gaussian function by a complex exponential function. Fig. 5 shows the Gabor wavelet used with its real part, imaginary part, and its low pass filter.

$$\psi(t) = \frac{1}{\sqrt{2\pi\sigma^2}} e^{-\frac{t^2}{2\sigma^2}} e^{i\omega t} \quad (1)$$

where,  $t$  denotes time,  $\sigma$  represents the standard deviation of the Gaussian function.  $\omega=2\pi f$ , where  $f$  is the center frequency of  $\psi$  and  $i$  is the imaginary unit. The Gabor complex wavelet's envelope is a low-pass filter, noted as  $\Phi$  in Eq. (2).

$$\Phi(t) = |\psi(t)| \quad (2)$$

The scattering network is consisting of three stages as shown in Fig. 6. In the WSN: the 0<sup>th</sup> order  $S_0$ , the signal with a low-pass filter  $\Phi$  was convolved to analyze the slow variations and amplitude in the signal, and provide good time resolution but poor frequency resolution. Moving to the 1<sup>st</sup> order  $S_1$ , a specific-scale wavelet is employed to scrutinize high-frequency components within the ECG segments. And, the 2<sup>nd</sup> order  $S_2$  was proceed to further extract complementary high-frequency components from the analyzed signal. This process enhances our understanding of ECG characteristics.

$$S_0x(t) = x(t) * \Phi \quad (3)$$

$$S_1x(t) = |x * \psi_{\sigma_1}| * \Phi \quad (4)$$

$$S_2x(t) = ||x * \psi_{\sigma_1}| * \psi_{\sigma_2}| * \Phi \quad (5)$$

$$Sx(t) = \{S_0, S_1, \dots, S_n\} \quad (6)$$

After applying the WSN with an invariance scale of 10 seconds and utilizing  $Q_1=8$  and  $Q_2=1$  as the quality factors for the 2 filter banks, a tensor of size 12x205 was obtained for each ECG segment. Fig. 7 shows the frequency bands of first and second filter banks.

In this tensor, columns correspond to the scattering paths within the network, while rows represent time windows. This showcases the WSN's capability to achieve a 59% dimensionality reduction.

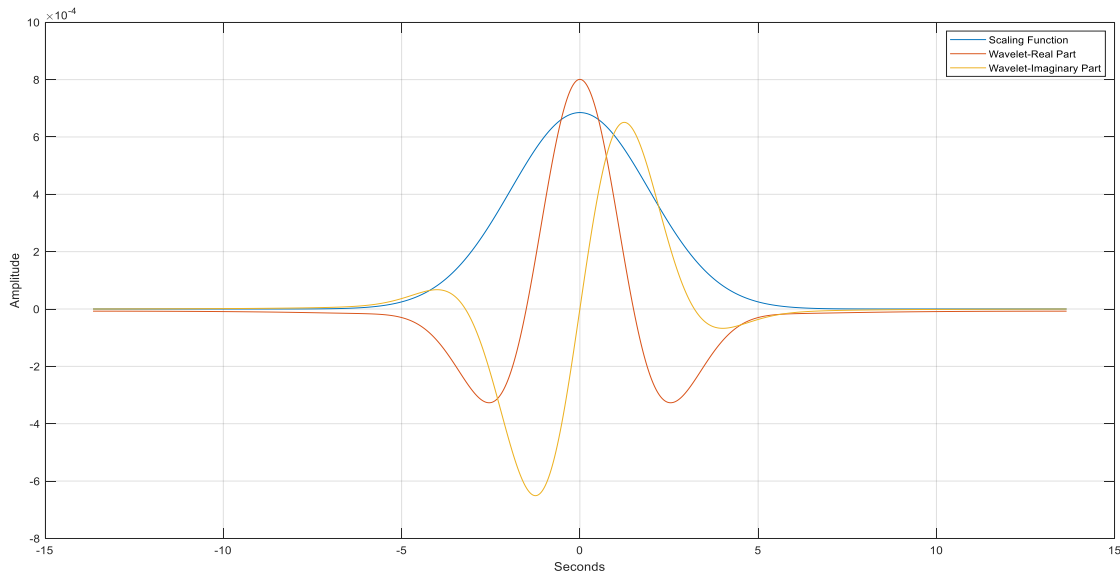


Fig. 5. Gabor complex wavelet.

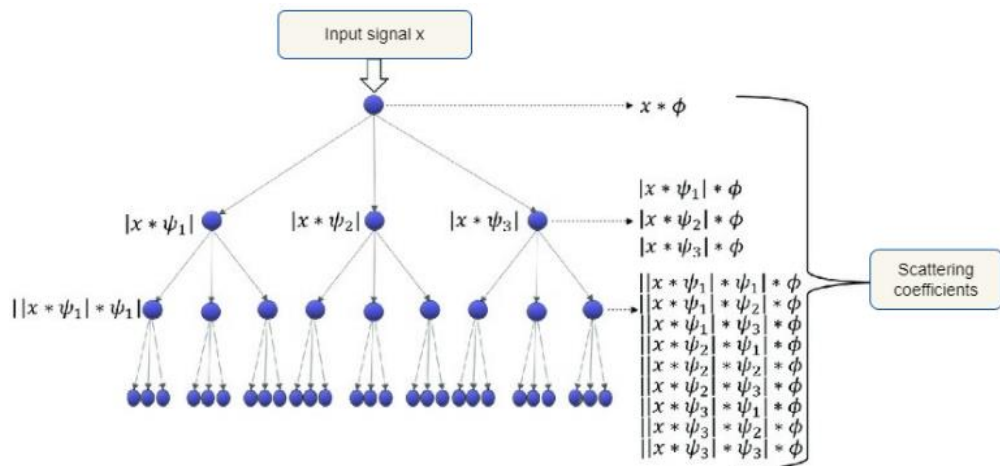


Fig. 6. Scattering network.

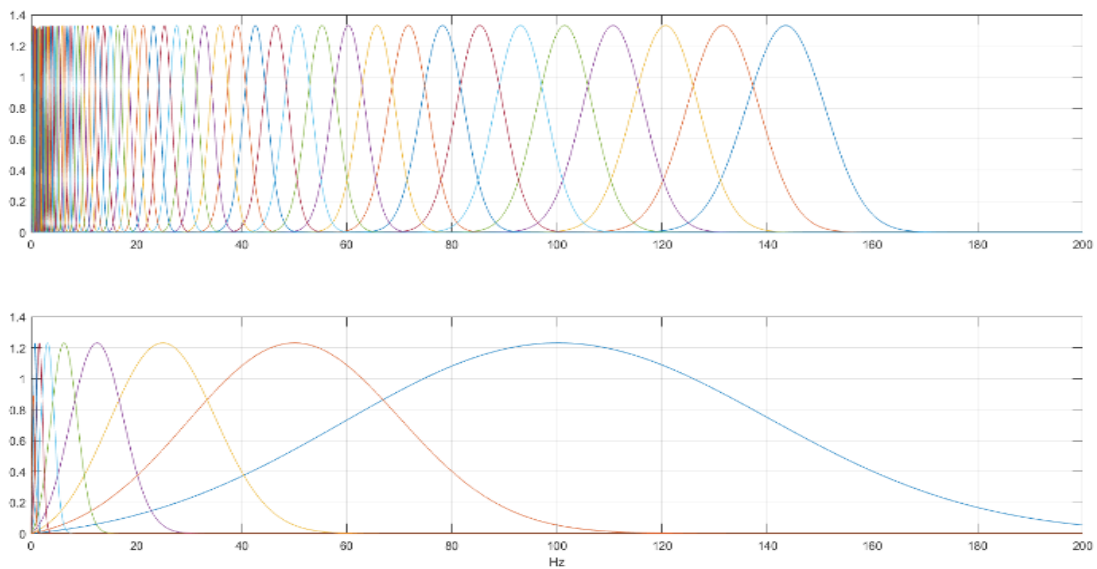


Fig. 7. Frequency band of the first and the second filter bank.

Consequently, the training dataset becomes 15065x12x205, and the testing dataset becomes 3764x12x205 in tensor dimensions. Subsequently, reshaping the training and testing datasets into an appropriate format for classifiers result in feature matrices of size 180780x205 and 45168x205 for training and testing, respectively.

The scalogram coefficients depicted in Fig. 8 showcase the outcomes of convolving the AF in ECG segment, as depicted in Fig. 1, with the real and imaginary components of Gabor wavelets within the initial filter bank.

This visual representation is exceptional in its ability to delineate the various frequencies present within the signal while associating each frequency with its respective temporal occurrence.

Moreover, the convolution process with these filters allows for the computation of similarity between the signal and the wavelets. These features are instrumental in providing insights into the amplitudes and frequencies within the signal, which in turn play a crucial role in accurately predicting atrial fibrillation.

The preceding WSN was implemented in the MATLAB environment, with an invariance scale set to 10 seconds and a sampling frequency of 300 Hz utilized.

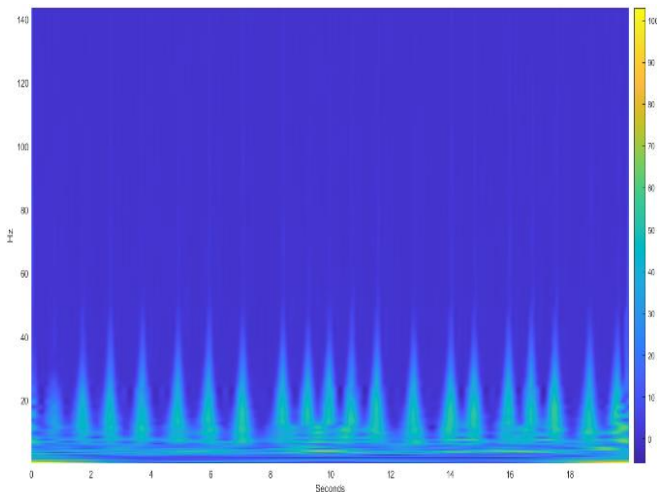


Fig. 8. Scalogram coefficients for the first filter bank.

#### D. Classification Model

In our study, an ANN was constructed with a single hidden layer containing 200 neurons. The goal was to effectively differentiate among classes A, N, O, and ~. The ReLU was used as activation function layer and Softmax as output activation layer. To enhance the model's performance, the Limited-memory-Broyden-Fletcher-Goldfarb-Shanno (LBFGS) solver was adopted, setting the maximum number of iterations to 1000. Throughout our analysis, we focused on refining the accuracy and efficacy of our approach.

The first hidden layer equation for each neuron j can be described as follows:

$$Z_j = \sum_{i=1}^n W_{ij} X_i + b_j \quad (7)$$

$$a_j = \max(0, Z_j) \quad (8)$$

where, n is the number of input features,  $W_{ij}$  is the weight between input features i and hidden neuron j,  $b_j$  is the bias term of hidden neurone j, and  $a_j$  is the output of neuron j after applying the ReLU activation function.

For each class c of the output layer:

$$Z_c = \sum_{j=1}^{200} W_{jc} a_j + b_c \quad (9)$$

$$Y_c = \frac{e^{Z_c}}{\sum_{k=1}^4 e^{Z_k}} \quad (10)$$

where,  $Y_c$  is the predicted probability for class c after applying the Softmax activation function.

The ANN was constructed within the MATLAB environment, with initial weights determined using the 'glorot' method and initial biases set to zeros. The maximum number of iterations was set at 1000, and the gradient tolerance was established as  $10^{-6}$ . The lambda parameter remained fixed at 0.

#### E. Evaluation Metrics

Our classifier model's performance was evaluated using metrics like accuracy, precision, recall, specificity, and the F1 score. Accuracy measures correct classifications, precision gauges accurate positive predictions, recall assesses positive instances captured, specificity measures accurate negative predictions, and the F1 score balances precision and recall.

**Accuracy:** It evaluates the ratio of accurate forecasts generated by the model among all the predictions it makes.

$$\text{Accuracy} = \frac{TP+TN}{TP+TN+FP+FN} \quad (11)$$

**Precision:** It evaluates how well the model correctly identifies positive cases, indicating the ratio of true positives to all positive predictions.

$$\text{Precision or PPV} = \frac{TP}{TP+FP} \quad (12)$$

**Sensitivity:** It measures the percentage of real positive instances accurately detected by the model and also referred as recall or the true positive rate.

$$\text{Recall or Sensitivity} = \frac{TP}{TP+FN} \quad (13)$$

**Specificity:** It evaluates the model's capability to correctly recognize negative cases through the measurement of true negative prediction's proportion.

$$\text{Specificity} = \frac{TN}{TN+FP} \quad (14)$$

**F1 Score:** It calculates a balanced evaluation of the model's performance by taking the harmonic mean of both precision and recall, merging them into a single metric.

$$\text{F1 score} = \frac{2 * \text{precision} * \text{sensitivity}}{\text{precision} + \text{sensitivity}} \quad (15)$$

#### F. System Description

The implementation of all algorithms was carried out using MATLAB version R-2021b on a Windows server. The system employed for execution featured an Intel (R), Core (TM), i5,

CPU 6300U, processor clocked at 2.40 GHz, with a 12 GB RAM capacity and operating on a 64 bits architecture.

#### IV. RESULTS AND DISCUSSION

##### A. Results

The objective of our paper was to classify ECG signals into four classes: AF, N, O, and ~. Numerous ML models were tested to assess their effectiveness in distinguishing these classes. Our findings, as indicated in Table II, revealed that an ANN with a single hidden layer and a size of 100 neurons yielded the best classification results. This architecture achieved an accuracy of 87.2% on the validation data and 81.1% on the testing data.

Interestingly, our observations also highlighted that increasing the size of the first hidden layer led to improved accuracy in both training and testing data. To delve deeper into this phenomenon, the impact of various hidden layer sizes was examined on classification outcomes. The results, depicted in Fig. 9, confirmed that accuracy consistently improved with larger layer sizes. However, it's important to note that excessively increasing the layer size can result in heightened computational costs and reduced prediction speed. Therefore, the layer size was adjusted at 200 neurons, which balanced accuracy and computational efficiency. With this configuration, a remarkable accuracy rates were achieved: 90.35% on the validation data and 82.10% on the testing data.

Upon applying the WSN to each ECG signal, a tensor of dimensions 12x205 was obtained. After reshaping the data for training and testing, an ANN was employed with a hidden layer size of 200. The ANN produced 12 results corresponding to different time windows. Consequently, each time window exhibited distinct validation and testing accuracies.

In Fig. 10, the impact of these time windows on validation and testing accuracy was analyzed. The results revealed that

the 5<sup>th</sup> time window yielded the highest classification performance, achieving 91.85% accuracy on validation data and 83.95% accuracy on testing data.

This proposed approach, known as Time Window Selection showcased a noteworthy enhancement in accuracy. Validation accuracy improved from 90.35% to 91.85%, while testing accuracy saw an increase from 82.10% to 83.95%.

Enhancing the testing accuracy is achievable through the strategic selection of optimal time windows for classification, followed by applying a majority vote approach. Fig. 10 illustrates that starting from the 3<sup>rd</sup> time window, there is a noticeable improvement in validation accuracy.

To harness this insight, the results from the ANN with a 200-layer size across 12-time windows were utilized, focusing on the 3<sup>rd</sup> through the 10<sup>th</sup> time windows, which displayed superior validation accuracy. Employing a majority vote technique on these eight selected time windows, we observed a significant enhancement in testing accuracy and F1 score.

TABLE II. PERFORMANCE COMPARAISON OF DIFFERENT MACHINE LEARNING MODELS

Models	Decision Tree	Narrow Neural Network layer size: 10	Medium Neural Network layer size: 25	Wide Neural Network layer size: 100	Bilayered Neural Network First layer size: 10 Second layer size: 10
Accuracy					
Validation Data %	61.8	75.2	80.2	87.2	75.8
Testing Data %	62.1	74.4	78.0	81.1	72.1

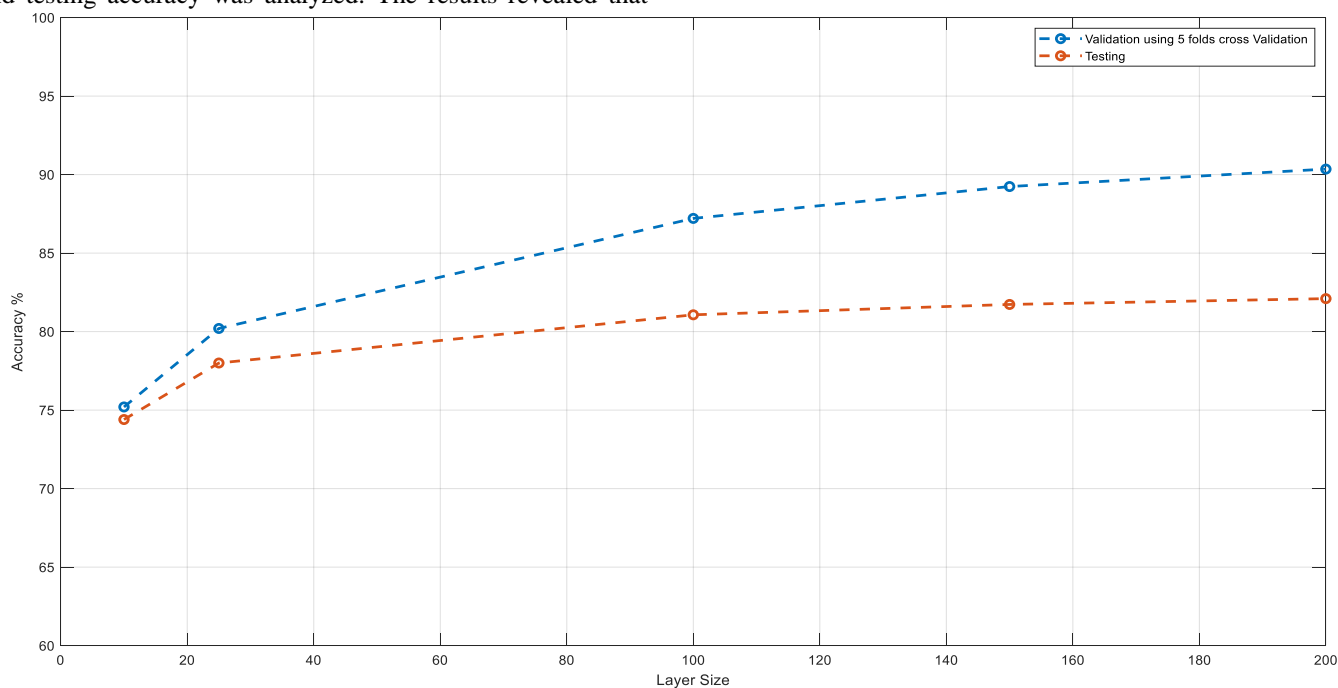


Fig. 9. ANN layer and its impact on validation and testing accuracy.

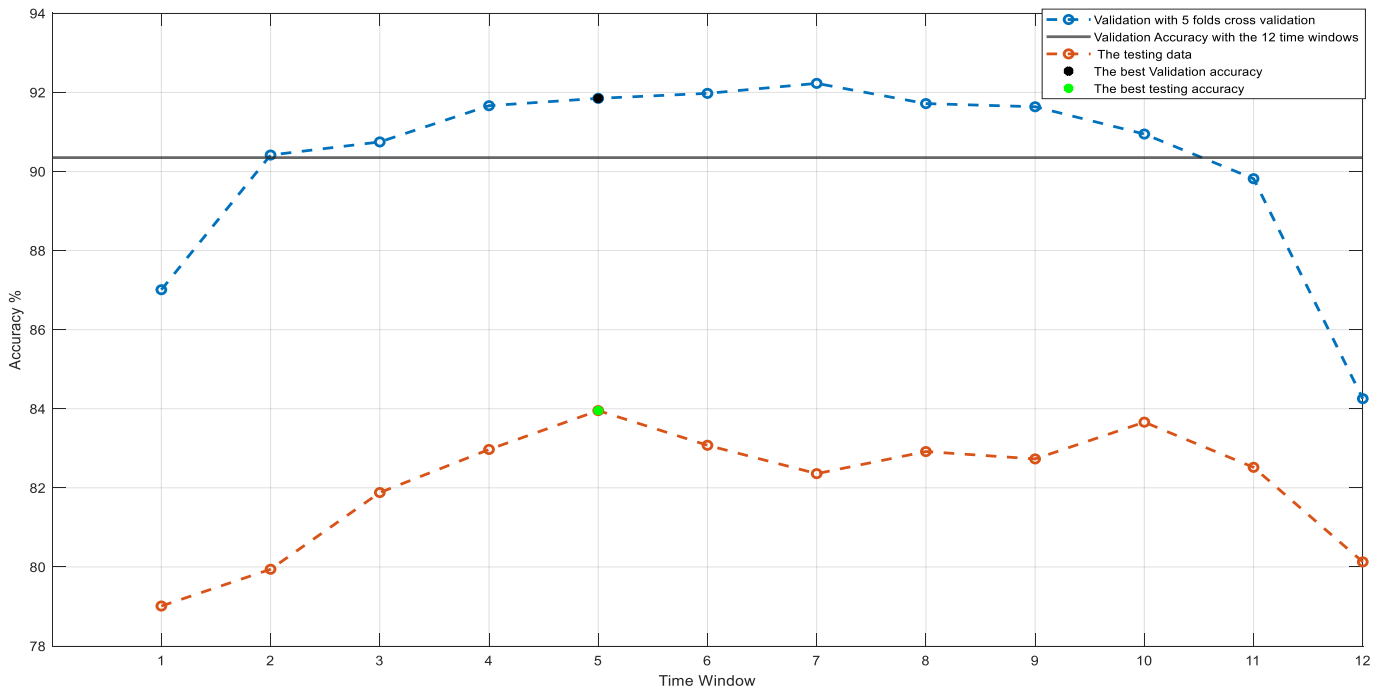


Fig. 10. Time windows impact on validation and testing accuracies.

TABLE III. TESTING RESULTS USING WSN + ANN + TIME WINDOWS SELECTION + MAJORITY VOTE

Class Name	Precision %	Recall %	Specificity %	F1 score %
AF	89.05	93.23	98.11	91.09
N	85.19	89.37	89.86	87.23
O	84.19	76.73	93.48	80.29
~	97.40	98.43	99.53	97.91
<b>Average</b>	88.96	89.44	95.24	89.13

TABLE IV. SUMMERIZED RESULTS ON THE VALIDATION AND THE TESTING DATASETS

	Methodology	Accuracy %	F1 score %
<b>5 Folds Cross Validation on the Training Dataset</b>	WSN + ANN with 12 Time window	90.35	91.53
	WSN + ANN + 5 <sup>th</sup> Time window	91.85	93.02
<b>Testing Dataset</b>	WSN + ANN with 12 Time window	82.10	84.22
	WSN + ANN + 5 <sup>th</sup> Time window	83.95	85.94
	WSN + ANN + Time Windows selection + Majority Vote	87.35	89.13

This approach led to a testing accuracy of 87.35% and an F1 score of 89.13%.

Detailed testing results are available in Table III, while Table IV provides a concise summary of the outcomes obtained through various methodologies.

Fig. 11 displays the various steps outlined in this paper for classifying ECG signals as N, AF, ~, or O.

### B. Discussion

In this study, we compared the outcomes produced by our classification method with those of previously established state-of-the-art models. Our model, which combines WSN, ANN, Time window, and Majority vote technique, achieves the highest overall accuracy. When contrasted with the findings of Pandey et al. [18], as presented in Table V, our model outperforms the state of art models in term of accuracy.

A comparative analysis of our results with those of other studies was conducted, specifically focusing on the F1 score.

The highest F1 score, 89.13%, was attained in our paper. Nonetheless, as shown in Table VI, it remains evident that our proposed methodology surpasses the performance of preceding works in terms of F1 score.

An extensive examination of the model's complexity was conducted, encompassing the neuron count in the ANN and the overall count of learnable parameters. Additionally, the time taken for feature extraction from a single ECG segment, quantified at approximately 67.3 milliseconds as displayed in Table VII. The predictive speed of our ANN successfully attains a rate of 22,584 ECG segments per second, showcasing a remarkably high prediction speed for detecting atrial fibrillation within ECG segments.

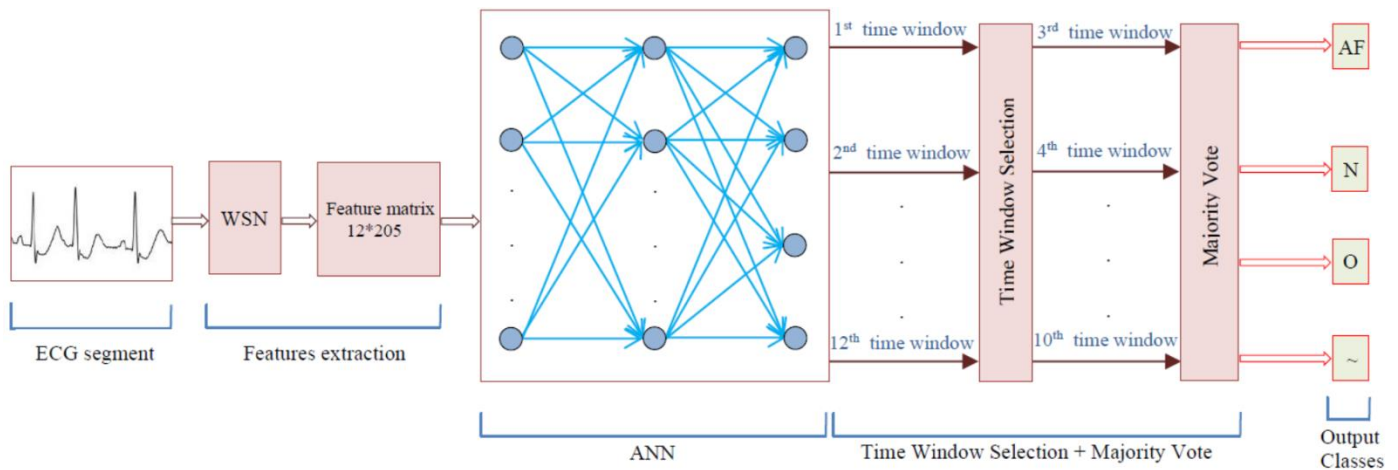


Fig. 11. ECG segments classification process.

TABLE V. OVERALL ACCURACY COMPARAISON WITH OTHER PREVIOUS WORK

Study	Methodology	Accuracy %
Pandey et al. [25]	<i>ResNet</i>	84.40
	<i>ResNet + LSTM</i>	82.87
	<i>ResNet + RBF</i>	84.56
Present Study	<i>WSN + ANN</i>	82.10
	<i>WSN + ANN + 5<sup>th</sup> Time window</i>	83.95
	<i>WSN + ANN + Time windows selection + Majority Vote</i>	<b>87.35</b>

TABLE VI. F1 SCORE COMPARAISON WITH OTHER PREVIOUS WORKS

Study	F1 score %
García et al. [18] (2017)	73
Rajpurkar et al. [19] (2017)	79.9
Coppola et al. [20] (2017)	78.55
Maknickas et al. [21] (2017)	78
Schwab et al. [22] (2017)	79
Jimenez-Serrano et al. [23] (2017)	77
Andreotti et al. [24] (2017)	79
Clifford et al. [26] (2017)	86.8
Pandey et al. [25] (2022)	80.56
Present Work (2023)	<b>89.13</b>

TABLE VII. COMPLEXITY ANALYSIS

No. Neurons	204
No. Learnables	42004
Feature Extraction Time for 1 ECG segment	67.3 millisecond
Prediction Speed of ANN	22584 ECG segment/s
Training Time	240.7 minutes

## V. CONCLUSION

In our research, an innovative approach for the automated classification of ECG signals and the detection of atrial fibrillation was presented.

Our technique leverages a combination of WSN with ANN, Time Windows Selection, and Majority Vote to yield promising results when compared to prior studies, achieving an accuracy of 87.35%, a precision of 88.96%, a recall of 89.44%, a specificity of 95.24%, and an F1 score of 89.13%.

Although, our proposed approach has shown a good performance, it still has some limitations. Firstly, the ANN performance was dependent on the accuracy and reliability of the features derived from the raw ECG data before being inputted. Secondly, the current method is challenged by a significant computational burden due to the feature extraction process.

In forthcoming work, we intend to explore a technique that mitigate the computational costs associated with our proposed model

To addressing these identified constraints, future endeavors will focus on enhancing the proposed model through the application of dimensionality reduction techniques utilizing machine learning. This enhancement aims to streamline the feature space, thereby lowering the computational load in the classification process without compromising the ANN efficacy.

## DATA AVAILABILITY

ECG readings were taken from: <https://archive.physionet.org/pn3/challenge/2017/>.

## CONFLICTS OF INTEREST

We confirm that all authors declare no conflicts of interest.

## ACKNOWLEDGMENT

This work was supported by the National Scientific and Technical Research Centre (CNRST), Morocco.

REFERENCES

- [1] J. Sundnes, G. T. Lines, X. Cai, B. F. Nielsen, K. A. Mardal, A. Tveito, "Computing the electrical activity in the heart," Springer Science & Business Media, (Vol. 1), 2007.
- [2] M. K. Islam, G. Tangim, T. Ahammad, M. R. H. Khondokar, "Study and analysis of ecg signal using matlab &labview as effective tools," International journal of Computer and Electrical engineering, 4(3), 404. 2012.
- [3] A. K. M. F. Haque, M. H. Ali, M. A. Kiber, M. T. Hasan, "Detection of small variations of ECG features using wavelet," ARPN Journal of Engineering and applied Sciences, 4(6), 27-30, 2009.
- [4] E. J. D. S. Luz, W. R. Schwartz, G. Cámara-Chávez, D. Menotti, "ECG-based heartbeat classification for arrhythmia detection: A survey," Computer methods and programs in biomedicine, 127, 144-164, 2016.
- [5] A. U. Rahman, R. N. Asif, K. Sultan, S. A. Alsaif, S. Abbas, M. A. Khan, A. Mosavi, "ECG classification for detecting ECG arrhythmia empowered with deep learning approaches," Computational intelligence and neuroscience, 2022.
- [6] S. S. Hussain, F. Noman, H. Hussain, C. M. Ting, S. R. G. S. bin Hamid, H. Sh-Hussain, ..., J. Ali, "A Brief Review of Computation Techniques for ECG Signal Analysis," In Proceedings of the Third International Conference on Trends in Computational and Cognitive Engineering: TCCE 2021 (pp. 223-234). Singapore: Springer Nature Singapore, February 2022.
- [7] L. Saclova, A. Nemcova, R. Smisek, L. Smital, M. Vitek, M. Ronzhina, "Reliable P wave detection in pathological ECG signals," Scientific Reports, 12(1), 6589, 2022.
- [8] R. Holgado-Cuadrado, C. Plaza-Seco, L. Lovisoló, M. Blanco-Velasco, "Characterization of noise in long-term ECG monitoring with machine learning based on clinical criteria," Medical & Biological Engineering & Computing, 1-14, 2023.
- [9] X. Dong, W. Si, "Heartbeat dynamics: a novel efficient interpretable feature for arrhythmias classification," IEEE Access, 2023.
- [10] V. Rawal, P. Prajapati, A. Darji, "Hardware implementation of 1D-CNN architecture for ECG arrhythmia classification," Biomedical Signal Processing and Control, 85, 104865, 2023.
- [11] M. Karri, C. S. R. Annavarapu, "A real-time embedded system to detect QRS-complex and arrhythmia classification using LSTM through hybridized features," Expert Systems with Applications, 214, 119221, 2023.
- [12] G.Y.H. Lip, L. Fauchier, S.B. Freedman, I. Van Gelder, A. Natale, C. Gianni, S. Nattel, T. Potpara, M. Rienstra, H. Tse, D.A. Lane, "Atrial fibrillation," Nature Reviews Disease Primers 2, 16016, 2016.
- [13] Developed with the Special Contribution of the European Heart Rhythm Association (EHRA), Endorsed by the European Association for Cardio-Thoracic Surgery (EACTS), Authors/Task Force Members, Camm, A. J., Kirchhof, P., Lip, G. Y., ... & Zupan, I. (2010). Guidelines for the management of atrial fibrillation: the Task Force for the Management of Atrial Fibrillation of the European Society of Cardiology (ESC). European heart journal, 31(19), 2369-2429.
- [14] R. Colloca, "Implementation and testing of atrial fibrillation detectors for a mobile phone application, 2013.
- [15] I. Savelieva, J. Camm, J., "Update on atrial fibrillation: part I," Clinical Cardiology: An International Indexed and Peer-Reviewed Journal for Advances in the Treatment of Cardiovascular Disease, 31(2), 55-62, 2008.
- [16] G. V. Naccarelli, H. Varker, J. Lin, K. L. Schulman, "Increasing prevalence of atrial fibrillation and flutter in the United States," The American journal of cardiology, 104(11), 1534-1539, 2009.
- [17] A. Ghrissi, D. Almonfrey, F., Squara, J. Montagnat, V. Zarzoso, "Identification of spatiotemporal dispersion electrograms in atrial fibrillation ablation using machine learning: A comparative study," Biomedical Signal Processing and Control, 72, 103269, 2022.
- [18] M. García, J. Ródenas, R. Alcaraz, J. J. Rieta, "Atrial fibrillation screening through combined timing features of short single-lead electrocardiograms," In 2017 Computing in Cardiology (CinC) (pp. 1-4). IEEE, September 2017.
- [19] P. Rajpurkar, A. Y. Hannun, M. Haghpanahi, C. Bourn, A. Y. Ng, "Cardiologist-level arrhythmia detection with convolutional neural networks," arXiv preprint arXiv:1707.01836, 2017.
- [20] E. E. Coppola, P. K. Gyawali, N. Vanjara, D. Giaime, L. Wang "Atrial fibrillation classification from a short single lead ECG recording using hierarchical classifier," In 2017 Computing in Cardiology (CinC) (pp. 1-4). IEEE, September 2017.
- [21] V. Maknickas, A. Maknickas, "Atrial fibrillation classification using qrs complex features and lstm," In 2017 Computing in Cardiology (CinC) (pp. 1-4). IEEE, September 2017.
- [22] P. Schwab, G. C. Scebbba, J. Zhang, M. Delai, W. Karlen, "Beat by beat: Classifying cardiac arrhythmias with recurrent neural networks," In 2017 Computing in Cardiology (CinC) (pp. 1-4). IEEE, September 2017.
- [23] F. Andreotti, O. Carr, M. A. Pimentel, A. Mahdi, M. De Vos, "Comparing feature-based classifiers and convolutional neural networks to detect arrhythmia from short segments of ECG," In 2017 Computing in Cardiology (CinC) (pp. 1-4). IEEE, September 2017.
- [24] S. Jiménez-Serrano, J. Yagüe-Mayans, E. Simarro-Mondéjar, C. J. Calvo, F. Castells, J. Millet, "Atrial fibrillation detection using feedforward neural networks and automatically extracted signal features," In 2017 Computing in Cardiology (CinC) (pp. 1-4). IEEE, September 2017.
- [25] S. K. Pandey, G. Kumar, S. Shukla, A. Kumar, K. U. Singh, S. Mahato, "Automatic Detection of Atrial Fibrillation from ECG Signal Using Hybrid Deep Learning Techniques," Journal of Sensors, 2022.
- [26] G. D. Clifford, C. Liu, B. Moody, H. L. Li-wei, I. Silva, Q. Li, ..., R. G. Mark, "AF classification from a short single lead ECG recording: The PhysioNet/computing in cardiology challenge 2017," In 2017 Computing in Cardiology (CinC) (pp. 1-4). IEEE. F1 score :0.868, September 2017.
- [27] A. L. Goldberger, L. A. Amaral, L. Glass, J. M. Hausdorff, P. Ivanov, R. G. Mark, ..., H. E. Stanley, "PhysioBank, PhysioToolkit, and PhysioNet: components of a new research resource for complex physiologic signals," circulation, 101(23), e215-e220, 2000.
- [28] N. V. Chawla, K. W. Bowyer, L. O. Hall, W. P0 Kegelmeyer, "SMOTE: synthetic minority over-sampling technique," Journal of artificial intelligence research, 16, 321-357, 2002.
- [29] J. Bruna, S. Mallat, « Invariant scattering convolution networks," IEEE transactions on pattern analysis and machine intelligence, 35(8), 1872-1886, 2013.
- [30] S. S. Goh, A. Ron, Z. Shen, "Gabor and wavelet frames," World Scientific, (Vol. 10), 2007.